PRAMANA
— journal of
physics

Vol. 54, No. 4
April 2000
pp. 589–602

Recent results from CERN SPS experiments and the future heavy ion programme

Y P VIYOGI
Variable Energy Cyclotron Centre, 1/AF, Bidhan Nagar, Calcutta 700 064, India
Email: viyogi@veccal.ernet.in

Abstract. We describe the important results from the recent experiments using lead beams at the CERN SPS. The results of the WA98 experiment, which has substantial Indian participation along with the photon multiplicity detector is described in some detail. Combining the preliminary results from various experiments looking at different signals of phase transition, one finds enough evidences to suggest that phase transition has taken place in nuclear collisions at the SPS. Future programme of heavy ion physics at the LHC is being geared around the ALICE experiment. This will comprise of detector subsystems capable of studying almost all the signals in the same event. The photon multiplicity detector will be an important component of the ALICE experiment, being a totally Indian contribution to ALICE.

Keywords. Quark-gluon plasma; photon multiplicity detector; disoriented chiral condensates, azimuthal anisotropy; flow; scaling; J/ψ suppression; strangeness enhancement.

PACS Nos 24.85.+; 25.75.-q

1. Introduction

In heavy ion collisions at ultra-relativistic energies one hopes to be able to create a high-density matter which existed for a fleeting moment in the early history of our universe, shortly after Big Bang. One expects that at the SPS energies the energy-density obtained in colliding heavy nuclei will surpass the critical density for color deconfinement (~ 1 GeV/fm^3). If such high energy densities can be obtained and the energy is sufficiently thermalised, strongly interacting matter will manifest itself as a quark-gluon plasma; the hadronic constituents become deconfined and hadrons lose their identity.

Several possible signatures have been proposed over the years to look for such a deconfined phase of matter. Attainment of thermalization has to be verified. The signals directly relating the observables of quark-gluon plasma phase have been: quarkonium suppression, strangeness enhancement, excess of direct thermal photons and continuum dileptons. Supporting evidences are also expected from the study of collective flow manifested by the attainment of thermalisation, properties of the interacting volumes at freezeout (size, lifetime, temperature) and multiplicity fluctuations arising due to critical phenomena at the phase boundary. In addition the deconfined matter may also have chiral symmetry restored. This will be reflected in the modifications of observed masses of vector mesons and in the formation of disoriented chiral condensates.

Table 1. List of heavy-ion experiments at the CERN SPS.

Expt.	Major equipments	Observables	Status
WA98	PMD/SPMD, LEDA, Plastic ball, MIRAC, ZDC, Goliath magnet, tracking chambers, TOF	$N_\gamma, N_{\rm ch}$, photon and charged particle, momentum spectra, transverse and forward energy, wide acceptance	completed
WA97 NA57	Si-pixel telescopes, multiplicity det. magnets, pad chambers	strange and multi-strange baryons and hyperons near mid-rapidity	relocated as NA57, continuing
NA49	TPC, Forward calori-meter, vertex magnet, TOF	momentum spectra of identified charged hadrons, wide acceptance	continuing
NA50	Muon tracking chambers pixel detectors, magnet	dimuon invariant mass spectra over a wide range	continuing
NA45	RICH, Si-drift, TPC	low mass dileptons	continuing
NA44	tracking chambers, magnets	identified charged hadrons, narrow acceptance	completed

The lead ion beam was made available to various experiments at the CERN SPS in October 1994 for the first time. A list of the experiments, along with major equipments and the observables they addressed, is provided in table 1. The emphasis in the design of the experiments has been complementarity rather than competition.

The WA98 and NA44 experiments finished data taking in 1996. All others have continued to take data. The WA97 experiment was relocated as NA57 experiment with Goliath magnet in north area beam lines. Analyses of data have been going on in various stages.

2. Results from SPS experiments

Several review articles summarise the results in comprehensive manner [1]. Here we shall describe the results from the WA98 experiment with special emphasis on PMD data. In addition we shall also briefly describe other important results like J/ψ suppression and strangeness enhancement.

The layout of the WA98 experiment is shown in figure 1 as a representative setup at the SPS. The experiment consists of sub-systems for measuring the momenta of identified charged hadrons using the GOLIATH magnet and a set of tracking chambers along with time-of-flight devices on both arms, photon momenta using highly segmented lead–glass calorimeter, multiplicities of photons and charged particles using higher granular detectors (PMD, SPMD, Si-drift) and the transverse and forward energy using MIRAC and ZDC calorimeters for centrality selection.

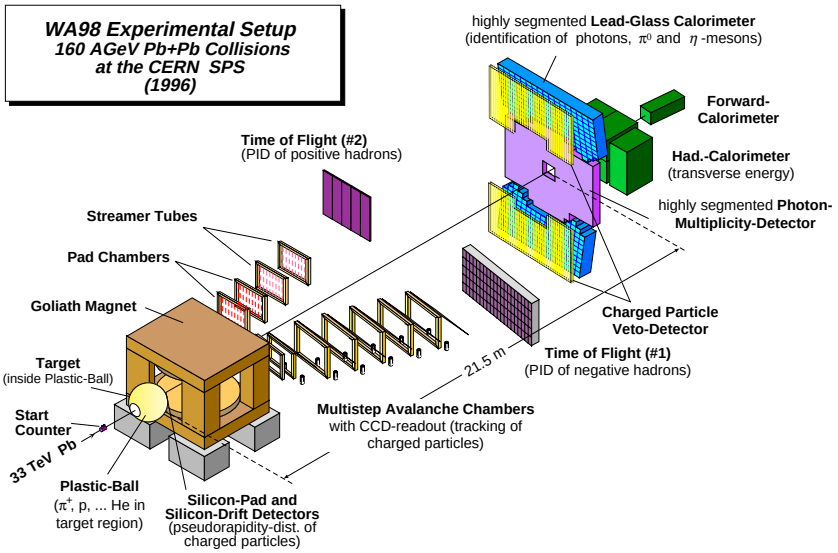

Figure 1. Layout of the WA98 experiment. The photon multiplicity detector was an Indian contribution.

2.1 *Photon multiplicity distributions*

Multiplicity and pseudorapidity distributions of photons have been measured using the PMD for different targets at 158 A.GeV beam energy [2]. The studies have also been made as a function of centrality. The minimum bias multiplicity distribution of photons is not explained by the VENUS event generator [3], the N_γ values are higher for the data compared to those of VENUS at the highest centralities.

The pseudorapidity density $\rho_{\max}$ and width σ of the Gaussian distribution fitted to the pseudorapidity distribution are shown in figure 2 as a function of the number of participants $N_{\rm part}$. This helps to combine the data from various targets. The $\rho_{\max}$ values increase monotonically with $N_{\rm part}$ while σ does not change with increasing $N_{\rm part}$.

Integrating the Gaussian fit parameters of the pseudorapidity distributions one can obtain the total number of photons over full phase space. Figure 2c shows the extracted values of $N_\gamma^{\rm tot}$ for Pb + Pb as a function of $N_{\rm part}$. The solid line shows a fit to the data using the function

$$N_\gamma^{\rm tot} = C\ .(N_{\rm part})^\alpha, \tag{1}$$

where C is a proportionality constant. The value of the exponent α is extracted to be 1.12±0.03. This is in excellent agreement with those derived for neutral pions [4]. By dividing the phase space into two parts, one corresponding to the central rapidity region ($2.4 \leq \eta \leq 3.4$) and the other beyond this we find that α = 1.12 for both the regions in the data. In comparison fitting the photon distribution from the VENUS event generator in the above two regions yields different exponents, 1.10 at mid-rapidity and 1.0 in the outside region.

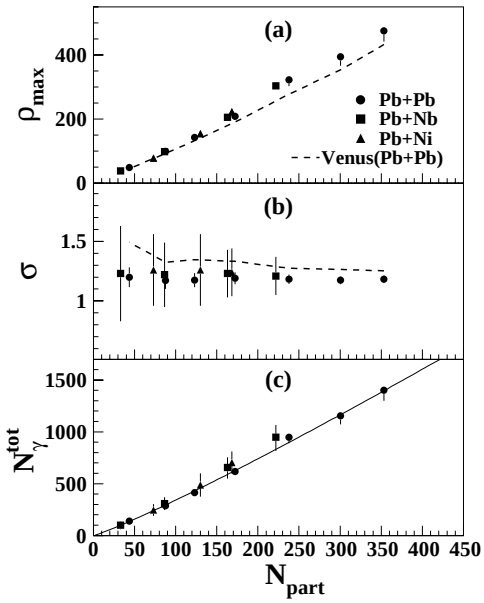

Figure 2. (**a**) Pseudorapidity density ($\rho_{\max}$), (**b**) width of the pseudorapidity distributions (σ), and (**c**) integrated values of number of photons ($N_\gamma^{\rm tot}$), as functions of the number of participant nucleons at different centrality bins for Pb induced reactions on Ni, Nb, and Pb targets at 158 A GeV. The solid line in (c) is a power-law fit to the data, which yields the value of the exponent, $\alpha = 1.12 \pm 0.03$.

The scaling exponent deviating from unity is thought to have its origin in the multiple scattering suffered by the partons [5].

2.2 *Azimuthal anisotropy and flow*

Colliding nuclear matter emerges with a flow pattern that has its origin in the amount of incompressibility of nuclear matter or in the effect of mean fields. A measurement of any section of the three-dimensional event shape reveals the momentum distribution at freezeout. Centrality dependence of flow is shown to be sensitive to the equation of state, and has been shown to have different behaviours for a hadron gas and a quark–gluon plasma [6–8].

Hydrodynamical models have shown that the magnitude of elliptic flow is sensitive to the initial spatial anisotropy and its subsequent evolution [9]. It is therefore desirable to measure the azimuthal anisotropy for different particle species in the final state. It is advantageous to study the event shapes with photons because their transverse distribution and that of the parent pions is not affected by the final-state Coulomb effects.

The WA98 and NA49 experiments have studied in detail the azimuthal anisotropy and collective flow using the Fourier analysis techniques for different particle species. The data

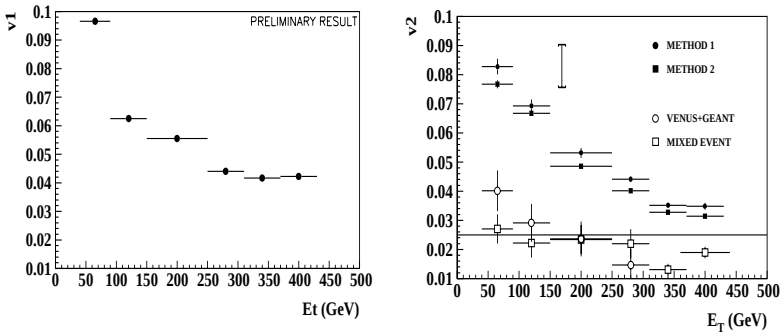

Figure 3. Left: Directed flow component v_1 as a function of centrality; right: elliptic flow component v_2 as a function of centrality.

from the PMD has already been used to study collective flow at the SPS energies [10] in sulphur induced reactions. We describe the flow results as obtained using the WA98 PMD.

The azimuthal distribution of photons can be described by a shape:

$$r(\phi) = \frac{1}{2\pi}\left[1 + 2v_1\cos(\phi - \psi_1) + 2v_2\cos 2(\phi - \psi_2)\right] , \tag{2}$$

where v_1 and v_2 denote the first and second order flow components corresponding to directed and elliptic flow respectively.

The azimuthal distribution is first corrected for detector artifacts by one of the established methods. The anisotropy parameters v_1 and v_2 are then calculated using the above relation on event-by-event basis and then the event averages for a given centrality are also computed. The details of data analysis can be found in ref. [22]. The results for both v_1 and v_2 are shown as a function of centrality (E_T) in figure 3. For comparison the results VENUS + GEANT and mixed events are shown in the figures. It is observed that the anisotropy in the data are much more than in the mixed event case. The anisotropy is larger in semi-central collisions than in central collisions. Further analysis of the data to understand the physical effects of the large anisotropy values is in progress.

2.3 *Disoriented chiral condensates*

The formation of hot and dense matter in high-energy heavy-ion collisions has the possibility of creating a chiral-symmetry-restored phase in the laboratory. After the initial stage of the collision, the system cools and expands leading to normal QCD vacuum in which the chiral symmetry is spontaneously broken. During this process, a metastable state may be formed in which the chiral condensate is disoriented from the true vacuum direction. This transient state would subsequently decay by emitting coherent pions within finite subvolumes or domains of the collision region. This possibility of the formation of the disoriented chiral condensate (DCC) would lead to large imbalances in the production of charged and neutral pions. This topic has initiated a lot of enthusiasm in terms of theoretical understanding [11] and experimental searches [12–14]. Although not conclusively explained,

the CENTAURO and anti-CENTAURO events observed in cosmic-ray experiments [15] remain possible candidates for large-scale charged-to-neutral fluctuations.

The primary signature of DCC is a large event-by-event fluctuation in photon to charged-particle multiplicity. This requires careful measurement of photons and charged particles in a common coverage. The PMD and the SPMD in the WA98 experiment measuring respectively the photon and charged particle multiplicities in a common coverage provide a good opportunity for DCC studies. Sophisticated analysis tools have been developed on an event-by-event basis to identify DCC amidst the large background due to conventionally produced particles [13,14,16–19].

The probability of distribution of the neutral pion fraction for the DCC case is given by

$$P(f) = \frac{1}{2\sqrt{f}} \qquad \text{where} \quad f = N_{\pi^0}/N_\pi \; . \tag{3}$$

N_{π^0} and N_π denote the number of neutral pions and total pions emitted from the domain, respectively. The pions in a normal event would follow a binomial distribution with a mean of 1/3. The formation of DCC would lead to event-by-event fluctuations in the number of charged particles and photons in a given phase space, since the majority of the photons originate from π^0 decay, and the contents of the charged particles are mostly charged pions.

The experimental observation of DCC depends on various factors, such as the probability of occurrence of DCC in a reaction, the number of possible DCC domains in an event, the size of the domains, the number of pions emitted from the domains, and the interaction of the DCC pions with the rest of the system. In view of this, specific analysis techniques have been devised to search for DCC. The current techniques in DCC analysis [14] are the following:

- N_γ *and* $N_{\rm ch}$ *correlation*: A simple method to study the correlation of the number of photons and charged particles in an event over the entire phase space covered by the detectors, and also in smaller $\eta - \phi$ bins.
- *Discrete wavelet analysis*: A multi-resolution analysis technique capable of picking up fluctuations at different $\eta - \phi$ bins of phase space.
- *Power spectrum analysis*: A method for identifying interesting events with DCC.
- *Robust observable*: A method using various moments and combinations of these, calculated from the distribution of photons and charged particles in each bin.

In a given set of normal events, the N_γ and $N_{\rm ch}$ distributions are correlated. The correlation between observed $N_{\gamma-{\rm like}}$ and $N_{\rm ch}$ can be studied using full detector coverage and also in smaller ϕ-segments. The widths of the S_Z distributions (as defined in ref. [13]) can be compared for data, mixed events and for the case of event generators folded with the detector response (VENUS + GEANT). The presence of events with DCC domains of a particular size would result in a broader distribution of S_Z compared to those for normal events when studied in ϕ-segments comparable with domain size. Preliminary results for the r.m.s deviations of the S_Z distributions for 2, 4, 8 and 16 bins in ϕ obtained for Pb+Pb collisions at 158 A GeV/c are shown in the left panel of figure 4. The data are compared to mixed events and event generator results.

The r.m.s values for the event generator are small due to impact parameter correlations between N_γ and $N_{\rm ch}$. The r.m.s values for mixed events are closer to those of data but a difference of two standard deviations persists. The results are being checked.

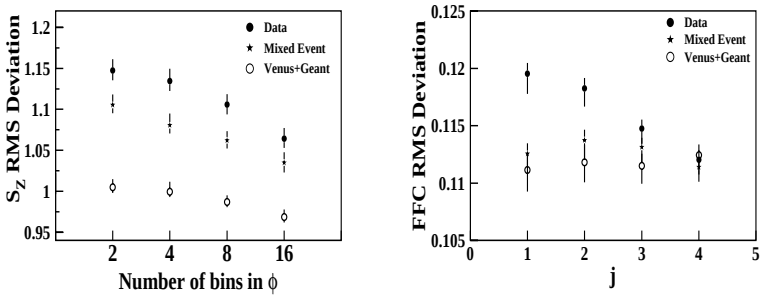

Figure 4. Left: S_Z rms deviation; right: FFC rms deviation.

The correlation at smaller ϕ-bins can also be studied using the method of discrete wavelet transformation (DWT). The ability of this technique to search for localized DCC domains has been demonstrated in refs [20,18].

The phase space of the PMD and the SPMD is divided into small bins in ϕ, the number of bins in a given scale j being 2^j. The input to the DWT analysis is a spectrum of f at the smallest bin, corresponding to the highest resolution scale, $j_{\max}$. The output of the DWT consists of a set of wavelet or father function coefficients (FFCs) at each scale, from $j = 1$,...,$(j_{\max} - 1)$.

The distribution of FFCs for normal events is Gaussian in nature. The presence of DCC-like fluctuation makes the FFC distribution non-Gaussian, with a larger r.m.s. deviation [18]. Comparing the r.m.s. deviations of the FFC distribution of data, mixed, and simulated events, one can get an idea about the localized fluctuations in the distributions of $N_{\gamma-\mathrm{like}}$ and N_{ch}. This is shown in the right panel of figure 4. Here again the data differs from the mixed events at intermediate ϕ-bins. Both these results suggest the presence of DCC-like fluctuation in azimuthal domains around 50–60 deg. Further checks are in progress.

2.4 *Direct photons*

Direct thermal photons emitted from the early stage of the plasma provide one of the most important signals of phase transition. Photon emission in ultra-relativistic nuclear collisions is dominated by the background from decay photons and hence the experimental search for thermal photons becomes very difficult. In spite of this difficulty, WA80 collaboration has made a concerted effort to measure the single photons and an upper limit to the emission of thermal photons was set by detailed analysis of the data and consideration of various systematic errors [21]. The upper limit was able to rule out the hadronic scenario of emission of photons unless one takes recourse to unphysical initial parameters.

The WA98 lead glass spectrometer is designed for the study of single photons. The analysis of the data is still in progress, but preliminary results do suggest that a significant excess production of single photons, over and above those expected from hadronic processes, is taking place. Figure 5 shows the results as a function of p_T for both peripheral and central collisions. Whereas the data for peripheral collisions are consistent

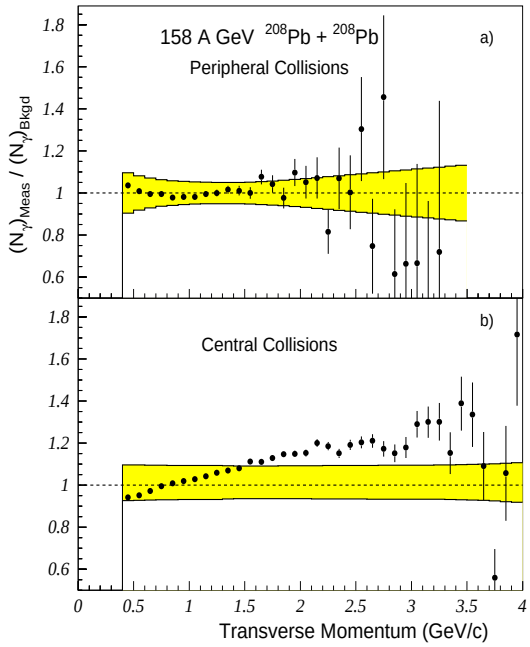

Figure 5. Preliminary result on direct single photons from WA98 experiment.

with hadronic emission (background), the results for central collisions indicate excess in the p_T window of 1.5 to 3.5 GeV/c. If confirmed, this should constitute one of the most important results suggesting that the phase transition is taking place in lead–lead collisions at the SPS energy.

2.5 *Other results*

Strangeness enhancement: In pp collisions the production of particles containing strange quarks is strongly suppressed due to the higher mass of strange quarks. In a QGP the $s\overline{s}$ pair can be formed copiously by gluonic interactions. Hence the yields of strange and multi-strange mesons and baryons has been predicted to be strongly enhanced in the QGP scenario as compared to hadron gas [23].

The strangeness fraction $\lambda_s = 2\langle\overline{s}s\rangle/(\langle\overline{u}u\rangle + \langle\overline{d}d\rangle)$ in nucleon–nucleon collisions is found to be 0.2–0.25. In contrast in heavy ion collisions the strangeness fraction λ_s is found to be 0.4–0.45. All known microscopic kinetic models based entirely on pp input and hadronic re-interaction dynamics fail to reproduce the strangeness enhancement. Heavy ion reactions thus generate a prehadronic state with different dynamics (presumably a longer life time) than in pp collisions.

The global strangeness enhancement reflected in λ_s occurs already in S + S collisions and remains roughly unchanged in Pb + Pb collisions. A recent comparison of p + Pb and

Pb + Pb collisions at the SPS [24] further shows that while the bulk of strangeness enhancement is carried by the kaons and hyperons (Λ, Σ), which are enhanced by a factor 3 near mid-rapidity, the enhancement is much stronger for the doubly and triply strange baryons Ξ and Ω and their anti-particles, with an enhancement factor of about 17 for $(\Omega + \overline{\Omega})$ at mid-rapidity. WA97 experiment also found [24] that all of the enhancement factors in Pb + Pb are independent of the collision centrality, i.e., of the size of the mid-rapidity source, from about 100 to 400 participating nucleons, and that similar enhancement patterns are seen in S + S collisions.

J/ψ suppression: One of the oldest proposed signatures of deconfinement in QCD at high densities and temperatures is the suppression of heavy quarkonia mesons [25]. At high densities, Debye screening in a QGP reduces the range of attractive force between heavy quarks and anti-quarks and beyond some critical density screening prevents the formation of bound states.

The NA38 experiment first reported J/ψ ($c\overline{c}$ pair) suppression in sulphur induced reactions [26]. However these data could be explained by hard QCD processes extrapolating from pA results. A rescaling of the data from different projectile target and energy combinations in lighter systems produces a universal curve $(AB)^{0.92}$, where A and B are the target and projectile masses. The recent results from Pb + Pb data on J/ψ suppression however are well below such a universal curve [27]. In addition it is interesting that this suppression pattern follows the binding energies of the corresponding charmonium states: suppression of the more strongly bound states requires a higher density and/or lifetime of the fireball. This anomalous suppression has generated lot of interest.

At present the suppression mechanism is not fully understood theoretically, but one condition appears to be unavoidable: strong rescattering of the $\overline{c}c$ pair in a very dense environment, probably of partonic origin.

3. ALICE : Heavy ion experiment at the LHC

The large hadron collider (LHC) will provide collisions of heavy ions at c.m. energy of 5.5 A TeV and is expected to be commissioned by the year 2005. The community of experimental physicists currently engaged in SPS experiments have collectively proposed a dedicated heavy ion experiment nick-named ALICE (A Large Ion Collider Experiment) [28]. The ALICE experiment will be capable to address all the diverse physics issues of nuclear collisions at ultra-relativistic energies.

3.1 *General description*

The layout of the ALICE experiment is shown schematically in figure 6. This will be located in point 2 intersection of the LEP tunnel, currently housing the L3 experiment. The L3 magnet will form one of the basic components of the ALICE experiment. The central barrel part of the detector will consist of an inner tracking system (ITS) followed by a time projection chamber (TPC), a transition radiation detector (TRD), a time-of-flight detector (TOF). Part of the barrel will also house a photon spectrometer (PHOS) and a high momentum particle identification (HMPID) setup.

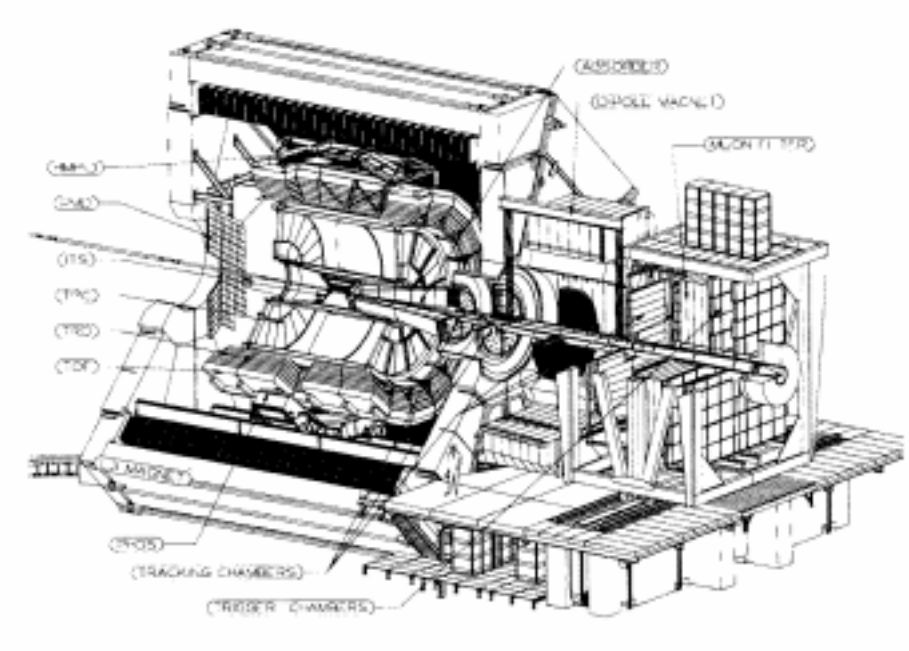

Figure 6. Layout of the ALICE experiment.

The forward region will have a dimuon spectrometer on one side and a photon multiplicity detector (PMD) on the other side. The dimuon spectrometer extends beyond the L3 magnet, it has a dedicated dipole and five stations of tracking chambers, a thick muon filter and two sets of trigger chambers. On the PMD side, a CASTOR calorimeter is proposed to look for exotic Centauro type events. On both sides of the interaction point there will be two zero degree calorimeters (ZDC) for tagging the centrality of collision.

3.2 *Signals and observables in ALICE*

The ALICE experiment is well designed to study almost all the signals proposed for the detailed investigation of quark-gluon plasma phase. In addition special effects expected at the LHC energy like minijets will also be studied.

The ITS, TPC, TRD, TOF and the HMPID systems together constitute an excellent assembly to identify and measure the momenta of charged hadrons from a few hundreds of MeV/c to several GeV/c in the pseudorapidity range $(-1, 1)$. In addition the PHOS photon spectrometer will be able to measure the momenta of photons in the mid-rapidity region and study the production mechanism of neutral mesons and single photons in the same way as done in the WA80 and WA98 experiments. The TRD having the capability of identifying high momentum electrons will add to the study of di-lepton production in the mid-rapidity region complementing the muon spectrometer in the forward region.

The muon spectrometer in the forward region will be dedicated to the study of quarkonium suppression. With 10 tracking planes in five stations and two trigger planes it will

have adequate mass resolution to study the various resonant states near υ family, which are bottomonium products.

In the forward region opposite to the muon spectrometer, highly granular preshower photon multiplicity detector (PMD) will be able to study collective flow, production of DCCs and multiplicity fluctuations.

The multiplicities of produced particles in nuclear collisions at the LHC will be very high, almost 8000 per unit of pseudorapidity at midrapidity. This will be useful in a new era of single event physics where observables will be extracted in each event without adding the effects over many events.

3.3 *Photon multiplicity detector*

Introduction: The PMD in ALICE will have full azimuthal coverage in the pseudo-rapidity region $1.8 \leq \eta \leq 2.6$. It will be mounted on the L3 magnet door 5.8 m from the interaction point [29].

Figure 7 shows the cross-section and layout of the PMD schematically. The veto detector in front of the converter is used to reject charged particles. Both the preshower and the veto detectors are based on a honeycomb proportional chamber design. There are $\sim 2 \times 10^5$ cells in the entire detector, each cell having an area of 1 cm^2. The honeycomb wall forms a common cathode, operated at a high negative voltage. The signal is read out from the anode wires at ground potential using GASSIPLEX front-end electronics [30]. The basic parameters of the PMD are given in table 2.

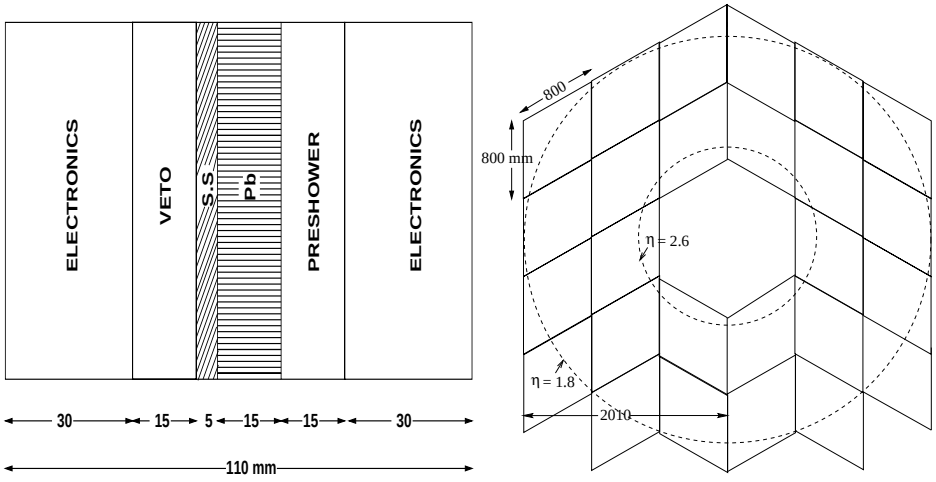

Figure 7. Left: Cross-section of the PMD (schematic only) showing the veto plane, lead converter and the preshower plane. SS is the support plate on which lead plates and chambers will be mounted. Right: The layout and the pseudorapidity coverage. Each rhombus denotes a supermodule of side 80 cm containing 72 × 72 hexagonal cells. The detector has a vertical axis of symmetry and the two halves can be opened independently.

Table 2. Basic parameters of the PMD.

Parameter	Value
Distance from vertex	580 cm
η-coverage	1.8–2.6
Active area	10 m^2
Inner radius	85 cm
Outer radius	200 cm
Cell size (area)	1 cm^2
Cell depth (gas depth)	8 mm
Number of channels	200,000

The honeycomb geometry is selected because of its closeness to a circular approximation, providing almost circular equipotentials within a cell. This geometry also facilitates close packing of large arrays. The same design can be used for both the preshower part and the charged-particle veto. The operating gas in the chamber is selected to be a mixture of Ar and CO_2 because of its insensitivity to neutrons and its non-inflammable nature.

Physics capabilities: The performance of the PMD has been simulated for various event centralities in Pb+Pb collisions and also using various physics processes relevant for the PMD-related signals.

The reconstruction of photons is done by clustering the hits on the preshower plane. Hadrons are rejected by employing a neural-network algorithm using signals in both the veto and preshower planes. The main results on the performance of the detector are given below.

- The efficiency of the PMD for counting photons has been estimated using simulations. For central Pb+Pb collisions we obtain values of 73% and 68%, respectively, for the cases of PMD only and with all detectors and beam pipes in the actual ALICE environment. The corresponding values of the purity of the photon sample are 75% and 61%.
- The PMD can provide an estimate of $E_T^{\rm em}$. The resolution of the e.m. transverse energy determined using the PMD ($\hat{E}_T$) for the entire PMD acceptance is $\sim$ 3% for fixed multiplicity. The fractional change in $\hat{E}_T$ obtained using the preshower signal is found to be $\sim$ 50% of the change in the transverse energy in the event.
- It is possible to discern the anisotropy of the event shapes in the ALICE environment for anisotropies as low as $\sim 2\%$ [31]. One can estimate the flow signal in the parent pions by measuring the signal in photons. The estimated flow does not significantly depend on the photon counting efficiency so long as the multiplicity is reasonably high. The resolution correction factor for the determination of event planes approaches unity for the multiplicities expected to be encountered in central Pb+Pb collisions within the PMD acceptance. The determination of the event plane will enable an investigation of any correlated emission of other particle species in different phase-space regions.
- The PMD can study event-by-event pseudorapidity fluctuations using the power spectrum technique. It will be possible to select events having non-statistical fluctuations at the 1% level of admixture in normal events. Multiplicity fluctuations of

photons for different impact parameters and colliding systems can be determined to a high accuracy.

- It is possible to detect signals of the formation of DCC primarily in conjunction with the FMD and also with other central detectors. Sophisticated analysis methods using wavelet techniques, robust observables and power spectrum have already been developed and shown to be sensitive to an identification of DCC signals.

4. Summary

The recent data from various experiments at the SPS, although preliminary in nature, collectively suggest that a deconfined phase of matter has been probably produced. Data analysis in progress will have to further confirm this early hint. Better microscopic understanding of the deconfined phase will further help to conclusively interpret the results as coming from the phase transition of hadronic matter and rule out the hadronic scenarios.

The WA98 experiment has made significant contribution to QGP studies and related physics topics. The PMD has emerged as an important subsystem capable of studying flow, DCC and fluctuations.

The ALICE subsystems are well designed for future studies at the LHC where one will be able to study almost all the signals of QGP in the same event. The PMD will remain an integral component of this experiment contributing to many areas of QGP studies.

References

[1] S A Bass, M Gyulassy, H Stocker and W Greiner, *J. Phys*. (1998) hep-ph/9810281
John Harris and Berndt Muller, *Ann. Rev. Nucl. Part. Sci.* **46**, 71 (1996)
J Alam, S Raha and B Sinha, *Phys. Rep.* **273**, 243 (1996)
[2] WA98 Collaboration: M M Aggarwal *et al*, *Phys. Lett.* **B458**, 422 (1999)
[3] K Werner, *Phys. Rep.* **232**, 87 (1993)
[4] WA98 Collaboration: M M Aggarwal *et al*, *Phys. Rev. Lett.* **81**, 4087 (1998)
[5] D K Srivastava, private communications
[6] W Reisdorf and H G Ritter, *Ann. Rev. Nucl. Part. Sci.* **47**, 663 (1997)
[7] P Danielewicz, e-print Nucl-th/9907098
[8] D H Rischke, *Nucl. Phys.* **A610**, 88c (1996)
J Y Ollitrault, *Nucl. Phys.* **A638**, 195c (1998)
[9] S A Voloshin and A M Poskanzer, e-print Nucl-th/9906075
[10] WA93 Collaboration: M M Aggarwal *et al*, *Phys. Lett.* **B403**, 390 (1997)
[11] J D Bjorken, *Int. J. Mod. Phys.* **A7**, 4198 (1992)
J D Bjorken, K L Kowalski and C C Taylor, SLAC-PUB-6109, Apr. 1993
A A Anselm and M G Ryskin, *Phys. Lett.* **B266**, 482 (1991)
J -P Blaizot and A Krzywcki, *Phys. Rev.* **D46**, 246 (1992)
K Rajagopal and F Wilczek, *Nucl. Phys*. **B399**, 395 (1993)
Masayuki Asakawa, Zheng Huang and Xin-Nian Wang, *Phys. Rev. Lett.* **74**, 3126 (1995)
Jorgen Randrup and Robert L Thews, *Phys. Rev.* **D56**, 4392 (1997)
[12] Minimax Collab.: T C Brooks *et al*, *Phys. Rev.* **D55**, 390 (1997)
[13] WA98 Collaboration: M M Aggarwal *et al*, *Phys. Lett.* **B420**, 169 (1998)
[14] WA98 Collaboration: T K Nayak *et al*, Quark Matter '97 proceedings, *Nucl. Phys.* **A638**, 249c (1998)

[15] C M G Lates, Y Fujimoto and S Hasegawa, *Phys. Rep.* **65**, 151 (1980)
[16] WA98 Collaboration: T K Nayak *et al*, PANIC '99 proceedings, *Nucl. Phys.* in press
[17] B K Nandi, Ph.D. Thesis, Utkal Univ. (1999)
[18] B K Nandi *et al*, *Phys. Lett.* **B461**, 142 (1999)
[19] D S Mukhopadhyay, Ph.D. Thesis, Univ. of Calcutta (1999)
[20] Zheng Huang, Ina Sarcevic, Robert Thews and Xin-Nian Wang, *Phys. Rev.* **D54**, 750 (1996)
[21] WA80 Collaboration: R Albrecht *et al*, *Phys. Rev. Lett.* **76**, 3506 (1996)
[22] G C Mishra, Thesis, Utkal Univ. Bhubaneswar (1999)
[23] J Rafelski, *Phys. Rep.* **88**, 331 (1982)
[24] WA97 Collaboration: E Anderson *et al*, *Phys. Lett.* **B433**, 209 (1998)
[25] T Matsui and H Satz, *Phys. Lett.* **B178**, 416 (1986)
[26] O Drapier *et al*, *Nucl. Phys.* **A544**, 209c (1994)
[27] NA50 collaboration: L Ramello *et al*, *Nucl. Phys.* **A638**, 261c (1998)
[28] ALICE Collaboration: Technical Proposal, CERN/LHCC/95–71 (1995)
[29] Photon Multiplicity Detector Technical Design Report, CERN/LHCC 99-32 (1999)
[30] ALICE HMPID Technical Design Report, CERN/LHCC 98-19 (1998)
J C Santiard *et al*, ALICE Internal Note, under preparation
[31] R Raniwala, S Raniwala and Y P Viyogi, ALICE Internal Note 99-32 (1999)